KSME Journal, Vol. 8, No. 3, pp. 283~292, 1994

On the Positioning of Control Sources in Active Noise Control of Three-Dimensional Interior Space

Oh-Sang Kwon,* Bong-Ki Kim and Jeong-Guon Ih****

(Received December 14, 1993)

Locations of secondary sources in three-dimensional active noise control influence greatly on final control result. To find efficient secondary source sites for given primary source layout, an acoustic analysis of a three-dimensional interior space is done for low frequency ranges with low modal density. By using the boundary element method, magnitude and phase of optimum velocities of boundaries are evaluated for underdetermined system with an example of a rectangular box. Because the potential energy at mutiple field points depends on boundary velocity field, "good" sites for control sources can be determined by investigating the distribution of resultant velocity vectors. Results show a general tendency that the dipole positioning is most effective and the source should be placed at antinodes of related modes for maximum noise reduction, and this agrees with previous ones. With this method, positions of control sources for maximum noise attenuation can be determined for a variety of primary source configurations and for irregular boundary shapes.

Key Words: Active Noise Control, Secondary Source, Source Position, Underdetermined System, Acoustic BEM, Optimal Velocity Field

1. Introduction

After several pioneering works (for instance, Olson and May, 1953; Jessel, 1972), active noise control(ANC) technique has been developed drastically due to the fast evolution of digital signal processing microprocessors during these 10 years. Majority of research works has been devoted to the control of one-dimensional duct system, and the control of the three-dimensional acoustic field has been studied for relatively recent days (Tichy, 1991). For ANC of the three-dimensional space, the control actions can be categorized into two strategies: local and global field control. Local control scheme produces a controlled field at several points but can possess adverse effects at other locations in general. By the global control of the field, the acoustic potential energy of the entire system can be reduced, which is an ultimate target for general noise control (Manginate, 1977). Most of the 3-D ANC has been done as local control and their problem is often the level of approximation to global control action. Piraux and Nayrole (1980) suggested a basic formula for analyzing the 3-D ANC problem by using a minimization technique of the squared pressure in an arbitrary domain, and this concept is equal to minimizing energy quantities in the field. Nelson et al. (1987), Bullmore et al. (1987), and Elliott et al. (1987) showed that the global control within a finite frequency band can be approximately realized by locating error microphones at antinodal positions of related acoustic modes. A series of analytical and experimental results (Nelson et al., 1987a; Nelson et al. 1987b; Bullmore et al., 1987; Elliott et al., 1987) gave excellent perspective for a basic understanding of the limitations and principles of active control in enclosures, but their modal method has weakness in applying it to general unknown

*Kia Motor Co., Kyoungki-do

**Department of Mechanical Engineering, Korea Advanced Institute of Science and Technology, Science Town, Taejon 305-701

modal fields and those with high modal densities. Recently, they have considered the problem of active minimization of total power output and maximizing the power absorption of the secondary sources for an array of controllable secondary sources and an array of original primary sources (Elliott et al., 1991). A consistent formulation was developed for the problem by using acoustic radiation and transfer impedances in an arbitrary three-dimensional environment. Mollo and Bernhard (1987) developed a method for minimizing the squared pressure by using the indirect boundary element method. They used velocity boundary conditions and a monopole control source in the field. Later, they also developed a formula including the signal from a detect microphone considered as a new noise source and their approach is just obtaining source strength of each point source (Mollo and Bernhard, 1990). Similarly, Cunefare and Koopmann (1991) also utilized the boundary element method for global noise control of radiated sound field. They regarded a part of boundaries as noise sources and concluded that the use of multiple control speakers will yield promising result based on examples for exterior field of radiating sphere and rectangular box interior. Until these days, practical applications are limited only to cases of low modal density with small modal overlap. Consequently, relatively small enclosures such as automobile cabins can be treated at the moment (Elliott et al., 1988; Guicking and Bronzel, 1990).

In this paper, efficient locations of secondary sources with finite size will be investigated by using the direct boundary element method (Brebbia, Telles, and Wrobel, 1984) for an enclosed sound field. Possible locations for secondary sources are limited only on the boundary surfaces. By categorizing the control source locations into several regimes and considering underdetermined control situation, "good" sites for control are rank-ordered through an example of a rectangular box with known acoustic modal characteristics at low frequencies. Acoustic potential energy is evaluated at some multiple interior field points to approximate a global control situation. The results presented will be for single frequency control at a number of frequencies in the chosen range, as is normally done in the practical active noise control system in automotive interiors.

2. Theoretical Model

2.1 General formulation

For harmonic pressure variations of p, the homogeneous acoustic field without flow of the medium is governed by the linearized Helmholtz equation. This can be transformed into the Kirchhoff-Helmholtz integral equation by using the Green's theorem as follows (Baker and Copson, 1939):

$$c(r)p(r)=\int_{so}[(\partial G/\partial n)\,p(r_0) - G(\partial p(r_0)/\partial n)]dS, \quad (1)$$

where $c(r)$ is 4π for interior points, 2π for boundary points, and 0 for exterior ones for smooth boundaries. Here, r is the observation point, r_0 means the source on the boundary, S denotes the boundary surface, and G is defined as free-space Green's function. For three-dimensional space, the Green's function, G, is given by

$$G=\exp(-ikR)/R;\ R=|r-r_0|, \quad (2)$$

where k means the wave number, R is the distance between observation and boundary points, and $i=\sqrt{-1}$.

Numerical integration should be done to evaluate Eq. (1) for irregularly shaped domains, and the boundary surfaces are discretized for this purpose. If the acoustic pressure is assumed constant in each discretized element, Eq. (2) can be rewritten as follows:

$$c_j p_j=-\sum_{m=1}^{Nele} p_m\int_{S_m}\left(\frac{1}{R_{jm}}+ik\right)\frac{e^{-ikR_{jm}}}{R_{jm}}\cos\theta_{jm}dS_m + i\omega\rho\sum_{m=1}^{Nele} v_m\int_{S_m}\frac{e^{-ikR_{jm}}}{R_{jm}}dS_m, \quad (3)$$

where S_m means the area of each boundary element, θ_{jm} describes the angle between observation point j and boundary element m, N_{ele} denotes the total number of discretized elements, ω is the circular frequency, and v_m indicates the surface

velocity on each element satisfying the Neumann boundary condition. By positioning r_j at the center of each element, one can define the two integrals in Eq. (3) as

$$D_{jm}=-\int_{Sm}\left(\frac{1}{R_{jm}}+ik\right)\frac{e^{-ikR_{jm}}}{R_{jm}}\cos\theta_{jm}dS_m$$

and $$M_{jm}=i\omega\rho\int_{Sm}\frac{e^{-ikR_{jm}}}{R_{jm}}dS_m, \tag{4}$$

where D is the dipole matrix and M is the monopole matrix. Then, Eq. (3) can be reexpressed by the following matrix equation:

$$[2\pi\delta_{jm}-D_{jm}]\{p_m\}=[M_{jm}]\{v_m\}$$
$$j=1,2,\cdots\cdots,\ \text{Nele} \tag{5}$$

where δ_{jm} represents the Kronecker delta. When $D'_{jm}=2\pi\delta_{jm}-D_{jm}$, and D'_{jm} is nonsingular, then

$$\boldsymbol{P}=\boldsymbol{D}'^{-1}\boldsymbol{M}\boldsymbol{V}. \tag{6}$$

Here, $\boldsymbol{P}$ and $\boldsymbol{V}$ means the acoustic pressure and the velocity vector on the boundary, respectively. Acoustic pressure in an interior three-dimensional space can be derived as follows:

$$\hat{\boldsymbol{P}}=\hat{\boldsymbol{D}}\boldsymbol{P}+\hat{\boldsymbol{M}}\boldsymbol{V}, \tag{7}$$

where the quantities in the interior space are denoted by caret symbol. By substituting Eq. (6) into (7), one obtains

$$\hat{\boldsymbol{P}}=\hat{\boldsymbol{D}}\boldsymbol{D}'^{-1}\boldsymbol{M}\boldsymbol{V}+\hat{\boldsymbol{M}}\boldsymbol{V}=\boldsymbol{Z}\boldsymbol{V}, \tag{8}$$

where $\boldsymbol{Z}=\hat{\boldsymbol{D}}\boldsymbol{D}'^{-1}\boldsymbol{M}+\hat{\boldsymbol{M}}$. In Eq. (8), the acoustic pressure at any interior points can be estimated if the velocity field on the boundary is thoroughly defined, so that the $\boldsymbol{Z}$ matrix can be regarded as a transfer matrix between the boundary velocity and the interior pressure field.

Acoustic potential energy approximated at finite number of points, N, is given by (Bullmore et al., 1987)

$$J_p=\frac{V}{4\rho c_0^2 N}\sum_{n=1}^{N}|\hat{p}_n|^2=A\sum_{n=1}^{N}|\hat{p}_n|^2, \tag{9}$$

where $A=V/(4\rho c_0^2 N)$, V is the volume of interior space, c_0 denotes the speed of sound in the medium, and ρ means the density of medium, or air in this paper. Substitution of Eq. (8) into (9) produces

$$J_p=A\hat{\boldsymbol{P}}^H\hat{\boldsymbol{P}}=A\boldsymbol{V}^H\boldsymbol{Z}^H\boldsymbol{Z}\boldsymbol{V}=\boldsymbol{V}^H\boldsymbol{B}\boldsymbol{V}, \tag{10}$$

where $\boldsymbol{B}=\boldsymbol{A}\boldsymbol{Z}^H\boldsymbol{Z}$, and the superscript H indicates Hermitian transpose. It can be noted that the approximated acoustic potential energy in Eq. (10) is expressed by the boundary velocity only.

2.2 Classification of boundary characteristics

In active noise control for an interior space, the boundary surface can be categorized into two parts, each representing the control source and the rest as vibrating sources, respectively. Thus, the boundary velocity field can be classified into the following two regimes assuming no sources inside the cavity:

$$\{V\}=\begin{Bmatrix}V_s\\V_p\end{Bmatrix}, \tag{11}$$

where V_p and V_s denote the velocity of vibrating primary noise source and of the rest as possible control sources, respectively. Substitution of Eq. (11) into (10) yields

$$\begin{aligned}J_p&=\begin{Bmatrix}V_s\\V_p\end{Bmatrix}^H\begin{bmatrix}\boldsymbol{B}_1&\boldsymbol{B}_2\\\boldsymbol{B}_3&\boldsymbol{B}_4\end{bmatrix}\begin{Bmatrix}V_s\\V_p\end{Bmatrix}\\&=\boldsymbol{V}_s^H\boldsymbol{B}_1\boldsymbol{V}_s+\boldsymbol{V}_p^H\boldsymbol{B}_3\boldsymbol{V}_s\\&\quad+\boldsymbol{V}_s^H\boldsymbol{B}_2\boldsymbol{V}_p+\boldsymbol{V}_p^H\boldsymbol{B}_4\boldsymbol{V}_P.\end{aligned} \tag{12}$$

This is a Hermitian quadratic form (Nelson et al., 1987) of $\boldsymbol{V}_s$ and the minimum potential energy can be determined by

$$\begin{aligned}\frac{\partial\boldsymbol{J}_p}{\partial\boldsymbol{v}_s}&=\boldsymbol{B}_1\boldsymbol{V}_s+\boldsymbol{B}_1^H\boldsymbol{V}_s\\&\quad+\boldsymbol{B}_3^H\boldsymbol{V}_p+\boldsymbol{B}_2\boldsymbol{V}_p=0.\end{aligned} \tag{13}$$

By utilizing the fact that $\boldsymbol{B}_1^H=\boldsymbol{B}_1$ and $\boldsymbol{B}_3^H=\boldsymbol{B}_2$, an optimal velocity field, $V_{s,\,opt}$, can be obtained as

$$\boldsymbol{V}_{s,opt}=-\boldsymbol{B}_1^{-1}\boldsymbol{B}_2\boldsymbol{V}_p, \tag{14}$$

which can be substituted into Eq. (12) to get the amount of potential energy after control process.

2.3 Underdetermined situation

The fore-going result is true as far as an overdetermined system is considered. However, when an underdetermined system is considered, the inverse of $\boldsymbol{B}_1$ matrix is not always exist. The following fact explains the cause of the phenomenon: the numerical singularity can be arisen when the field points of interest are clustered around some regions, and when the number of control sources is more than that of field points to be

controlled (Miyoshi and Kaneda, 1991; Elliott and Rex, 1992). Because "good" secondary source sites are being pursued in this paper, the latter situation corresponds to the system in question. In this study, the consideration of underdetermined system is only confined to developing a method of searching for effective secondary source sites by using boundary element method, not to developing practical controller with this underdetermined condition.

To solve the problem, a pseudoinverse of $\boldsymbol{B}_1$ matrix can be used instead of inverse matrix. By using the singular value decomposition (Forsythe, Malcolm, and Moler; 1977), the pseudoinverse of $\boldsymbol{B}_1$ is given by

$$\boldsymbol{B}_1^+ = \boldsymbol{R}\boldsymbol{\Sigma}^+\boldsymbol{L}^H, \tag{15}$$

where '+' symbol in the superscript denotes pseudoinverse, $\boldsymbol{R}$ is the right singular vector, $\boldsymbol{L}$ is the left singular vector, and $\sum$ means the diagonal matrix containing real positive sigular values. Then, the optimal velocity field and corresponding potential energy can be obtained as follows:

$$\boldsymbol{V}_{s,opt} = -\boldsymbol{B}_1^+\boldsymbol{B}_2\boldsymbol{V}_p, \tag{16}$$

$$\boldsymbol{J}_{p,opt} = \boldsymbol{V}_p^H\boldsymbol{B}_4\boldsymbol{V}_p - \boldsymbol{V}_p^H\boldsymbol{B}_3\boldsymbol{B}_1^+\boldsymbol{B}_2\boldsymbol{V}_p. \tag{17}$$

It is easy to show that $\boldsymbol{V}_{s,opt}$ is optimal solution for underdetermined case. To prove Eq. (16) to be optimal solution, Eq. (10) can be rewritten as follows:

$$J_p = \begin{Bmatrix} \boldsymbol{V}_s \\ \boldsymbol{V}_p \end{Bmatrix}^H \begin{bmatrix} \boldsymbol{B}_1 & \boldsymbol{B}_2 \\ \boldsymbol{B}_3 & \boldsymbol{B}_4 \end{bmatrix} \begin{Bmatrix} \boldsymbol{V}_s \\ \boldsymbol{V}_p \end{Bmatrix}. \tag{18}$$

If the singular value decomposition technique is applied to $\boldsymbol{B}_1$, then

$$\boldsymbol{B}_1 = \boldsymbol{V}_{B1}\boldsymbol{\Sigma}_{B1}\boldsymbol{V}_{B1}, \tag{19}$$

where $\boldsymbol{V}_{B1}$ is the right singular vector of $\boldsymbol{B}_1$ and $\boldsymbol{\Sigma}_{B1}$ means the diagonal matrix of singular values of $\boldsymbol{B}_1$. By combining Eqs. (18) and (19), one obtains a new expression of $\boldsymbol{B}$ matrix:

$$\boldsymbol{B} = \begin{bmatrix} \boldsymbol{V}_{B1} & \boldsymbol{O} \\ \boldsymbol{O} & \boldsymbol{I} \end{bmatrix} \begin{bmatrix} \boldsymbol{\Sigma}_{B1} & \boldsymbol{V}_{B1}^H\boldsymbol{B}_2 \\ \boldsymbol{B}_3\boldsymbol{V}_{B1} & \boldsymbol{B}_4 \end{bmatrix} \begin{bmatrix} \boldsymbol{V}_{B1}^H & \boldsymbol{O} \\ \boldsymbol{O} & \boldsymbol{I} \end{bmatrix}. \tag{20}$$

Resubstituting Eq. (20) into (18) leads to a revised form of potential energy expression as follows:

$$J_p = \begin{Bmatrix} \bar{\boldsymbol{V}}_s \\ \boldsymbol{V}_p \end{Bmatrix}^H \begin{bmatrix} \boldsymbol{\Sigma}_{B1}\bar{\boldsymbol{B}}_2 \\ \bar{\boldsymbol{B}}_2^H\boldsymbol{B}_4 \end{bmatrix} \begin{Bmatrix} \bar{\boldsymbol{V}}_s \\ \boldsymbol{V}_p \end{Bmatrix}, \tag{21}$$

where $\bar{\boldsymbol{V}}_s = \boldsymbol{V}_{B1}^H\boldsymbol{V}_s$ and $\bar{\boldsymbol{B}}_2 = \boldsymbol{V}_{B1}^H\boldsymbol{B}_2$. Some of diagonal elements of $\boldsymbol{\Sigma}_{B1}$ are zero for underdetermined system and $\bar{\boldsymbol{V}}_s$ can be classified into two parts: one is denoted by $\bar{\boldsymbol{V}}_{s1}$ which is a part of $\bar{\boldsymbol{V}}_s$ related with non-zero singular values, and another is designated by $\bar{\boldsymbol{V}}_{s2}$ related with zero singular values. Similarly, $\bar{\boldsymbol{B}}_2$ can be categorized into $\bar{\boldsymbol{B}}_{21}$ and $\bar{\boldsymbol{B}}_{22}$. Utilizing these, Eq. (21) can be expanded as

$$\begin{aligned} J_p = {} & \bar{\boldsymbol{V}}_{s1}^H\boldsymbol{\Sigma}_{B1}\bar{\boldsymbol{V}}_{s1} + \bar{\boldsymbol{V}}_{s1}^H\bar{\boldsymbol{B}}_{21}\boldsymbol{V}_p \\ & + \bar{\boldsymbol{V}}_{s2}^H\bar{\boldsymbol{B}}_{22}\boldsymbol{V}_p + \boldsymbol{V}_p^H\bar{\boldsymbol{B}}_{21}^H\bar{\boldsymbol{V}}_{s1} \\ & + \boldsymbol{V}_p^H\bar{\boldsymbol{B}}_{22}^H\bar{\boldsymbol{V}}_{s2} + \boldsymbol{V}_p^H\boldsymbol{B}_4\boldsymbol{V}_p, \end{aligned} \tag{22}$$

or, by considering input $\boldsymbol{V}_p$ and meaningful control source $\bar{\boldsymbol{V}}_{s1}$, one obtains

$$\begin{aligned} J_p = {} & (\boldsymbol{\Sigma}_{B1}^{1/2}\bar{\boldsymbol{V}}_{s1} + \boldsymbol{\Sigma}_{B1}^{-1/2}\bar{\boldsymbol{B}}_{21}\boldsymbol{V}_p)^H \\ & \times (\boldsymbol{\Sigma}_{B1}^{1/2}\bar{\boldsymbol{V}}_{s1} + \boldsymbol{\Sigma}_{B1}^{-1/2}\bar{\boldsymbol{B}}_{21}\boldsymbol{V}_p) \\ & - \boldsymbol{V}_p^H\bar{\boldsymbol{B}}_{21}^H\boldsymbol{\Sigma}_{B1}^{-1}\bar{\boldsymbol{B}}_{21}\boldsymbol{V}_p + \boldsymbol{V}_p^H\boldsymbol{B}_4\boldsymbol{V}_p \\ & + \bar{\boldsymbol{V}}_{s2}^H\bar{\boldsymbol{B}}_{22}\boldsymbol{V}_p + \boldsymbol{V}_p^H\bar{\boldsymbol{B}}_{22}^H\bar{\boldsymbol{V}}_{s2}. \end{aligned} \tag{23}$$

Optimal values of $\bar{\boldsymbol{V}}_{s1}$ and $\bar{\boldsymbol{V}}_{s2}$ minimizing J_p in Eq. (23) are

$$\bar{\boldsymbol{V}}_{s1} = -\boldsymbol{\Sigma}_{B1}^{-1}\bar{\boldsymbol{B}}_{21}\boldsymbol{V}_p \text{ and } \bar{\boldsymbol{V}}_{s2} = 0,. \tag{24}$$

where the corresponding minimum potential energy is given by

$$J_p = \boldsymbol{V}_p^H(\boldsymbol{B}_4 - \bar{\boldsymbol{B}}_{21}^H\boldsymbol{\Sigma}_{B1}^{-1}\bar{\boldsymbol{B}}_{21})\,\boldsymbol{V}_p. \tag{25}$$

Optimal $\bar{\boldsymbol{V}}_s$ composed of $\bar{\boldsymbol{V}}_{s1}$ and $\bar{\boldsymbol{V}}_{s2}$ can be reexpressed as follows:

$$\bar{\boldsymbol{V}}_s = \begin{Bmatrix} \bar{\boldsymbol{V}}_{s1} \\ \bar{\boldsymbol{V}}_{s2} \end{Bmatrix} = \boldsymbol{V}_{B1}^H\boldsymbol{V}_s = \begin{Bmatrix} -\boldsymbol{\Sigma}_{B1}^{-1}\bar{\boldsymbol{B}}_{21} \\ 0 \end{Bmatrix} \boldsymbol{V}_p, \tag{26}$$

or,

$$\begin{aligned} \boldsymbol{V}_S &= \boldsymbol{V}_{B1}^{H-1} \begin{bmatrix} -\boldsymbol{\Sigma}_{B1}^{-1}\bar{\boldsymbol{B}}_{21} \\ 0 \end{bmatrix} \boldsymbol{V}_p \\ &= -\boldsymbol{B}_1^+\boldsymbol{V}_{B1}\bar{\boldsymbol{B}}_2\boldsymbol{V}_p \\ &= -\boldsymbol{B}_1^+\boldsymbol{B}_2\boldsymbol{V}_p, \end{aligned} \tag{27}$$

Therefore, the velocity vector in Eq. (16) is proved as optimal vector.

If one considers an overdetermined system, secondary sources with large outputs are not necessarily the largest contributors to the resulting reductions in practice (Elliott et al., 1990). A poorly conditioned $\boldsymbol{Z}^H\boldsymbol{Z}$ matrix can result in large control effort on the part of some sources

with little benefit in terms of reductions. In the underdetermined case discussed in this paper, where every possible site on the boundary is effectively included, the assumption of "positions of elements with large magnitudes of $V_{s,opt}$ are possible sites for efficient noise control sources" is true as proved above. In other meanings, the abovementioned assumption is correct, because every possible transfer impedance between boundary and field points is included in the formulation for producing $V_{s,opt}$, and $V_{s,opt}$ is not just meaning the magnitude of source velocity but also implying the motional sensitivity of the boundary to field acoustic energy.

3. Simulation Results

In order to test the developed theory and concept, a rectangular box of 1.234 m×0.786 m×1.792 m(w×d×h) is adopted as shown in Fig. 1. The boundary surface is discretized into 104 constant elements as shown in Fig. 2 to make easy to excite any element as volume velocity source. The maximum characteristic length of each element is 0.45 m which limit the applicable high frequency range. This high frequency limit is about 125 Hz when the characteristic length corresponds to $\lambda/6$, and is about 200 Hz for $\lambda/4$ criterion with more numerical errors. Although the constant element seems to be a rough tool in calculation, it may be well to use this element type because the purpose of the paper is not to calculate exact magnitudes but to evaluate the relative magnitude of velocity field. Also, this element type has advantage in treating an element as a volume velocity source on average sense. For this rigid walled box without any acoustic damping, resonance frequencies can be obtained as shown in Table 1. Eight field points in the interior space are selected for evaluation or observation points, thus approximating the global control of the field. They are located near corners of the box and coordinates of those points are tabulated in Table 2.

Firstly, all the boundary elements are considered as control sources except no. 28 element which is only one primary noise source in the system. Element no. 28 located at a corner of xz-plane is selected as the noise source to excite all the acoustic modes efficiently. In Fig. 3, the potential energy of the uncontrolled and controlled state is compared to each other, which demonstrates that more than 70 dB of noise is

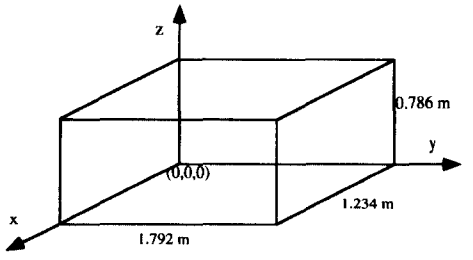

Fig. 1 Coordinates and dimension of rectangular box model for numerical simulations.

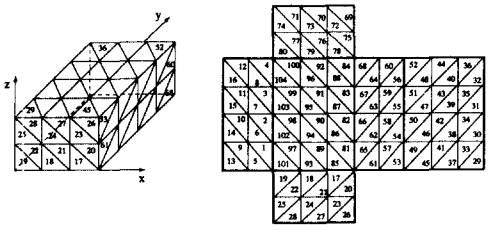

Fig. 2 Element numbering in boundary element simulations.

Table 1 Acoustic resonance frequencies and mode numbers of the rectangular box in Fig. 1.

No.	Frequency(Hz) (Exact)	N_x	N_y	N_z	Frequency(Hz) (BEM)
1	95.7	0	1	0	97
2	139.0	1	0	0	140
3	168.7	1	1	0	171
4	191.4	0	2	0	194
5	218.2	0	0	1	222

Table 2 Coordinates of field points for evaluating the acoustic potential energy (in meters).

No.	1	2	3	4	5	6	7	8
x	0.051	0.052	0.053	0.058	1.243	1.244	1.249	1.241
y	0.051	1.744	0.054	1.742	0.054	1.743	0.056	1.748
z	0.051	0.053	0.745	0.748	0.056	0.058	0.742	0.743

reduced for every frequency range of interest. Strictly speaking, maximum noise reduction can be attained by properly selected 8 control sources for 8 interested points, and additional control sources, e.g. 103 control sources in total, are redundant for practical purpose. However, the computation is performed here for finding most effective sites for control sources. When the underdetermined system is dealt with, the final controlled result can be made to zero or -∞ dB in theory (Nelson and Elliott, 1992). The residual noise in Fig. 3 is due to the truncation error in numerical computation. The dotted curve in Fig. 3 is the controlled result of an example of overdetermined case. Only the no. 29 element is used as a secondary source at which it is located as a dipole source.

In order to find optimal site for control source, a control source can be scanned over the whole boundary and the effect due to each configuration can be estimated. Then, this is equivalent to the technique using an overdetermined system. It can yield an effective result when the modeling of the noise source is well established, but the method includes a large amount of computation and one cannot assure that the position with maximum velocity is the optimal control source location. The purpose of the underdetermined model in this paper is to find the optimal secondary source positions considering the whole interior space.

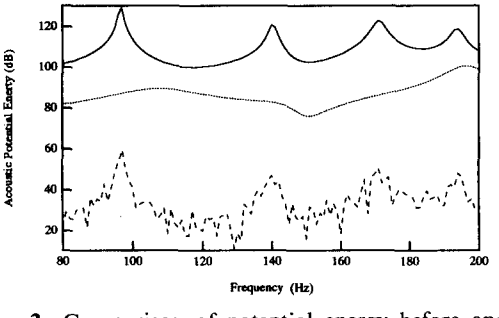

Fig. 3 Comparison of potential energy before and after control. In the after-control state, element no. 28 is primary noise source: _____, uncontrolled;·····, no. 29 element is control source (overdetermined system);------, all the elements except no. 28 are control sources (underdetermined system).

The starting point of the method is to investigate the magnitude of $V_{s,opt}$ of each boundary element as premised in the previous section. It is assumed and proved that the positions of elements with large magnitudes of $V_{s,opt}$, are possible sites for efficient control sources. One has to recall that $V_{s,opt}$ was estimated from the concept of transfer impedance by considering all the phase relationship between elements and/or field points.

Figure 4 shows the estimated distribution of $V_{s,opt}$ when no. 28 element in Fig. 2 is the primary noise source emanating 97 Hz sound. Positions at element nos. 13 and 29 possess distinguishably large values of velocities while 180° out-of-phase with primary source. These point are positioned very near to the primary source and at the corner of enclosure. In order to view an assembled state, Fig. 5 is retrofitted based on the data in Fig. 4. Figures 5(a) and 5(b) are unfolded view and Figs. 5(c) and 5(d) are assembled box in this condition. In Fig. 5 and subsequent similar figures, the phase other than 0° or 180° contains ambiguity due to the interpolation of data. One

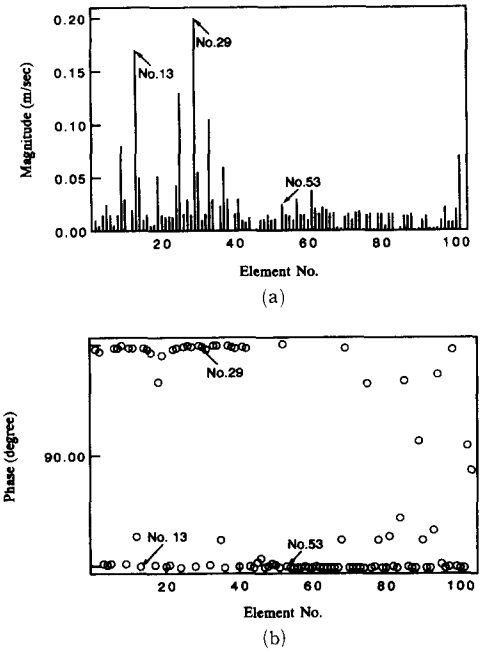

Fig. 4 $V_{s,opt}$ value at each element for 97 Hz when the primary noise source is located at element no. 28: (a) Magnitude; (b) Phase.

can conclude that the best control is expected when the control source is located very near to the primary source except at the antinode. This is the same conclusion drawn by Nelson et al. (1987). Positions at element nos. 13 and 29 are satisfying the rule and this also validates the assumption on the use of velocity amplitude in this section. Figure 6 is the result at 140 Hz, for which the primary source is located at element no. 28. One can observe a similar trend with Fig. 5. Most of the elements have 0° or 180° in phase. Several

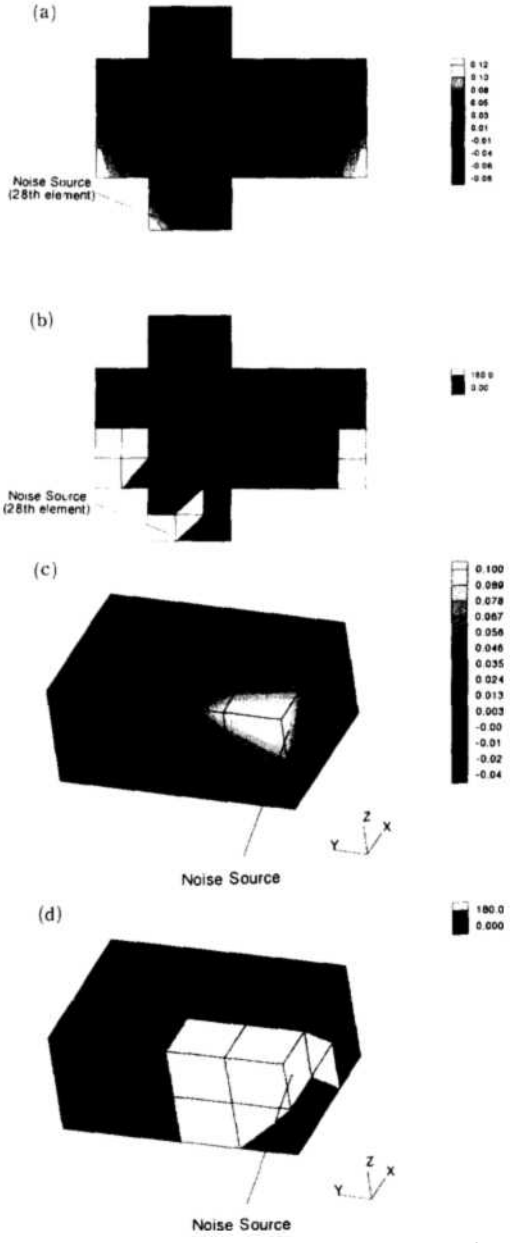

Fig. 5 Reconstructed view of $V_{s,opt}$ distribution in Fig. 4: (a), (b) Unfolded two-dimensional view according to the same configuration with Fig. 2; (c), (d) assembled three-dimensional view; (a), (c) Magnitude; (b), (d) Phase plot.

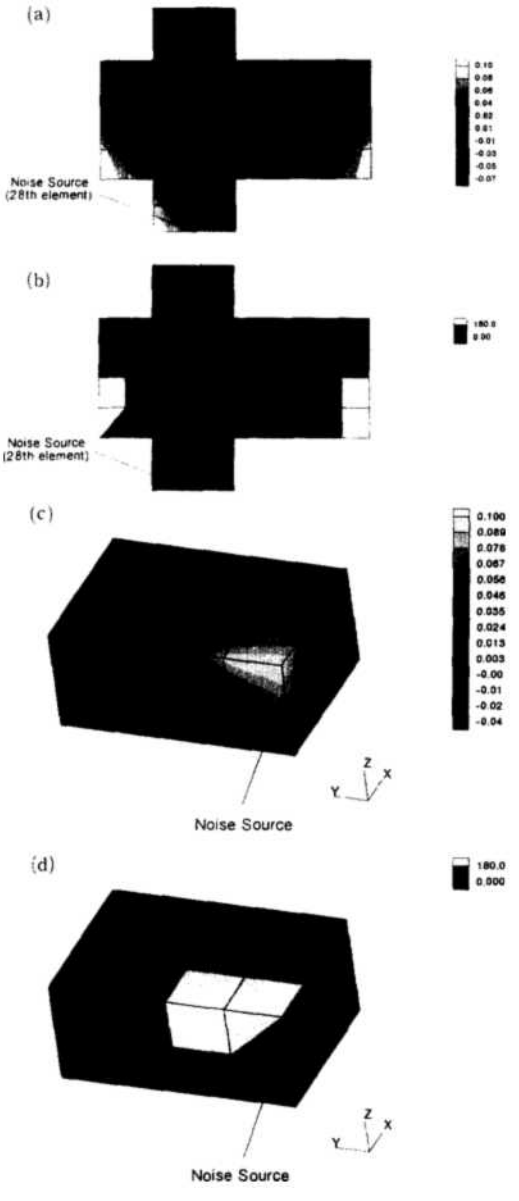

Fig. 6 $V_{s,opt}$ value at each element for 140 Hz when the primary noise source is located at element no. 28: (a), (c) Magnitude; (b), (d) Phase.

elements have phases other than 0° or 180°, but the magnitudes of their velocities are far smaller than others. The larger the magnitude, the phase has a trend of converging to 0° or 180°. For the foregoing two test frequencies, phase at element nos. 13 and 29 have 180° that the control effect can be called as dipole one considering the position of primary source very near to them.

The second situation is tested and the results are shown in Fig. 7 for two frequencies aforementioned. In this situation, the primary source is located at element no. 95 which is arbitrarily positioned near to the center of xy-plane. In Fig. 7(a) for 97 Hz, it is observed that the difference between magnitudes of velocities is not clear. Positions at element nos. 64, 67, 83, 87, 88 have nearly same amount of magnitudes, and the amplitude of element no. 91 is also similar to them. One can find in Fig. 7(c) that positions at element nos. 52 and 69 have predominantly large magnitudes of velocities for 140 Hz. The relative phase at the possible control source position is not sometimes 180° out-of-phase with primary source as can be seen in Fig. 8 for 140 Hz where element nos. 52 and 69 are in-phase with the primary noise source. This is due to the relatively long distance between secondary and primary source, which is in contrast with the dipole type configuration. Through this simple example, most effective positions for control sources can be pin-pointed by the analysis of underdetermined situations, as intended.

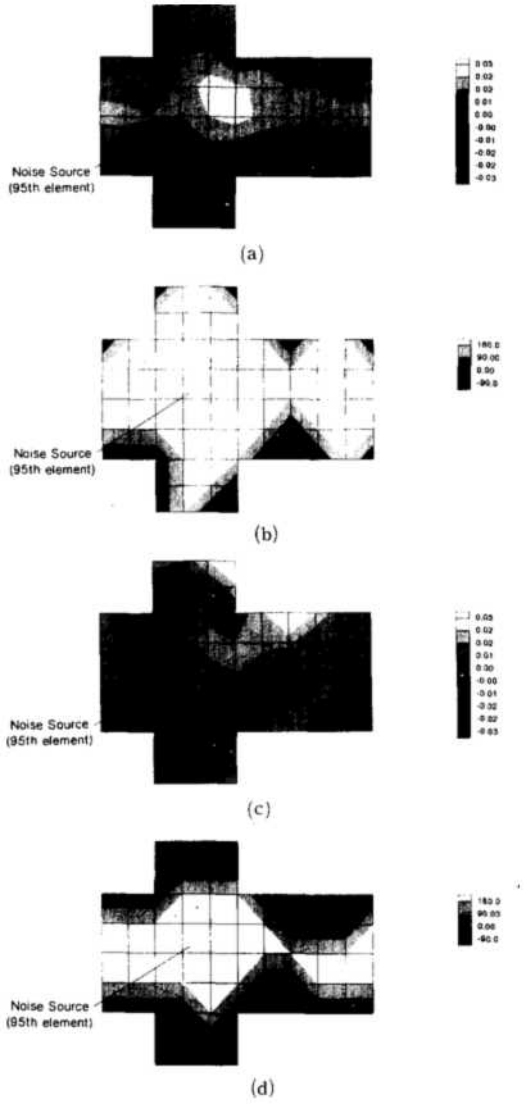

Fig. 7 $V_{s,opt}$ value at each element for 97 and 140 Hz when the primary noise source is located at element no. 95: (a), (b) 97 Hz; (c), (d) 140 Hz; (a), (c) Magnitude; (b), (d) Phase.

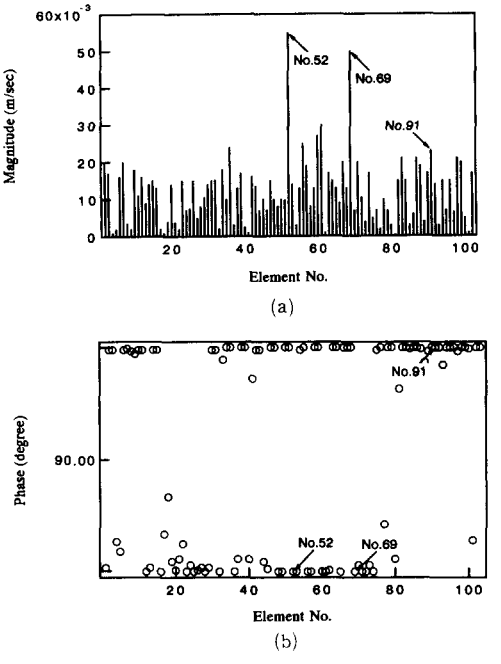

Fig. 8 $V_{s,opt}$ value at each element for 140 Hz when the primary noise source is located at element no. 95; (a) Magnitude; (b) Phase.

4. Concluding Remarks

The paper deals with a problem which has received an increasing degree of attention in recent days: namely, the selection of secondary source location in the three-dimensional interior space. In this paper, by using the boundary element method discretizing the Kirchhoff-Helmholtz equation for enclosed sound field, it is shown that the efficient sites for secondary noise sources can be determined, especially by considering the whole enclosure as an underdetermined system. The dipole effect of the coupled primary and secondary sources would be predominant for the efficient active noise control of the three-dimensional interior space. Most effective site of the control source is to be positioned that it is to very near to the primary source as well as on the antinode of the involved acoustic mode. This is the same conclusion drawn by the previous works (Elliott et al., 1991; Nelson and Elliott, 1992). Although the results are already conceived of in previous works, the purpose of this study is to establish a method to determine optimal positions of secondary sources for active noise control in irregularly shaped enclosures. With this method, most effective positions for control sources can be determined very easily for a given primary source layout, that the optimal control state can be simulated before practical installation and experiments.

In the aforementioned approach, the following aspects should be considered further: if the dipole matrix of the discretized Kirchhoff-Helmholtz equation is singular, the theory becomes meaningless. Numerical errors in the boudnary element computation can be appreciable, when the constant element is used as adopted in this study. As a cost function of the problem, acoustic potential energy evaluated and superposed at finite number of interior field points is selected. If the number of calculation points, N, is very large, then J_p in Eq. (9) can be approximately equal to the true global value. However, for practical computation purpose, the number of calculation points is to be limited that the result is not a true value in the rigorous meaning. In the underdetemined situation, the classification of the boundary surfaces by primary source and possible secondary one is not easy, although not impossible, in general. If some boundaries are vibrating more severely than others, one can consider those parts as primary sources. When the amplitude of vibration is nearly the same on all boundary surface, the classification is not so easy. This limitation can be a little bit relieved, if the primary source is determined to be the boundary surfaces where the practical control sources are not easy to install. For instance, it is very hard to install the secondary noise source at dash panels, floors, windshield, window, etc. in the passenger compartment of an automobile. Modeling technique using polypole (Kanai, Abe, and Kido, 1990; Nelson and Elliott, 1992) might be helpful for the further research on this aspect. In this study, the possible sites for secondary noise source are limited only to the boudary surface although some interior positions might be utilized for this purpose. Further study should be done also on this matter.

Acknowledgements

This work was supported partly by the Korea Science and Engineering Foundation(KOSEF).

References

Baker, B. B. and Copson, E. T., 1939, The Mathematical Theory of Huygens' Principle, Clarendon Press, Oxford.

Brebbia, C. A., Telles, J. C. F. and Wrobel, L. C., 1984, Boundary Element Techniques, Springer-Verlag, Berlin-Heidelberg.

Bullmore, A. J., Nelson, P. A., Curtis, A. R. D. and Elliott, S. J., 1987, "The Active Minimization of Harmonic Sound Field, Part II: A Computer Simulation," Journal of Sound and Vibration, Vol. 117, pp. 15~33.

Cunefare, K. A. and Koopmann, G. H., 1991, "A Boundary Element Approach to Optimization of Active Noise Control Sources on Three-Dimensional Structures," ASME Trans., Journal of Vibration and Acoustics, Vol. 113, pp. 387

~394.

Elliott, S. J., Curtis, A. R. D., Bullmore, A. J. and Nelson, P. A., 1987, "The Active Minimization of Harmonic Sound Field, Part III: Experimental Verification," Journal of Sound and Vibration, Vol. 117, pp. 35~58.

Elliott, S. J., Nelson, P. A., Stothers, I. M., Mcdonald, A. M., Quinn, D. C. and Saunders, T., "The Active Noise Control of Engine Noise inside Cars," 1988, Proceedings of Inter Noise 88, pp. 987~990.

Elliott, S. J., Nelson, P. A., Stothers, I. M. and Boucher, C. C., 1990, "In-flight Experiments on the Active Control of Propeller-induced Cabin Noise," Journal of Sound and Vibration, Vol. 140, pp. 219~238.

Elliott, S. J., Joseph, P., Nelson, P. A. and Johnson, M. E., 1991, "Power Output Minimization and Power Absorption in the Active Control of Sound," Journal of the Acoustical Society of America, Vol. 90, pp. 2501~2512.

Elliott, S. J. and Rex, J., 1992, "Adaptive Algorithms for Underdetermined Active Control Problems," Proceedings of International Conference on Acoustics, Speech, and Signal Processing (ICASSP), Vol. II, pp. 237~240.

Forsythe, G. E., Malcolm, M. A. and Moler, C. B., 1977, Computer Methods for Mathematical Computations, Prentice Hall, New York.

Guicking, D. and Bronzel, M., 1990, "Multichannel Broadband Active Noise Control in Small Enclosures," Proceedings of Inter Noise 90, pp. 1255~1258.

Jessel, M. J. M., 1972, "La Question des Absorbeurs Actifs," Revue d'Acoustique, Vol. 5, pp. 37~42.

Kanai, H., Abe, M. and Kido, K., 1990, "A New Method to Arrange an Additional Sound Source Used in Active Noise Control," Acustica, Vol. 70, pp. 258~264.

Mangiante, G. A., 1977, "Active Sound Absorption," Journal of the Acoustical Society of America, Vol. 61, pp. 1516~1523.

Miyoshi, M. and Kaneda, Y., 1991, "Active Control of Broadband Random Noise in a Reverberant Three-Dimensional Space," Noise Control Engineering Journal, Vol. 36, pp. 85~89.

Mollo, C. G. and Bernhard, R. J., 1987, "The Optimal Performance of Active Noise Controllers in Three Dimensional Cavities," SAE Paper 870994.

Mollo, C. G. and Bernhard, R. J., 1990, "Numerical Evaluation of the Performance of Active Noise Control Systems," ASME Trans., Journal of Vibration and Acoustics, Vol. 112, pp. 230~236.

Nelson, P. A., Curtis, A. R. D., Elliott, S. J. and Bullmore, A. J., 1987, "The Minimum Power Output of Free Field Point Sources and the Active Control of Sound," Journal of Sound and Vibration, Vol. 116, pp. 397~414.

Nelson, P. A., Curtis, A. R. D., Elliott, S. J. and Bullmore, A. J., 1987, "The Active Minimization of Harmonic Sound Field, Part I: Theory," Journal of Sound and Vibration, Vol. 117, pp. 1~13.

Nelson, P. A. and Elliott, S. J., 1992, Active Control of Sound, Academic Press, London.

Olson, H. F. and May, E. G., 1953, "Electronic Sound Absorber," Jouranl of the Acoustical Society of America, Vol. 25, pp. 1130~1136.

Piraux, J. and Nayroles, B., 1980, "A Theoretical Model for Active Noise Attenuation in Three Dimensional Space," Proceedings of Inter Noise '80, pp. 703~706.

Tichy, J., 1991, "Current and Future Issues of Active Noise Control," Journal of the Acoustical Society of Japan (E), Vol. 12, pp. 255~262.